Yuan, H., Li, Y., Jiang, J. Z., & Mellor, P. (2018). *Mechatronic Suspension Design for Vehicle Dynamic Performance Enhancement*. Paper presented at 28th International Conference on Noise and Vibration Engineering, ISMA2018 in conjunction with the 7th International Conference on Uncertainty in Structural Dynamics, USD2018, Leuven, Belgium.

Peer reviewed version

Link to publication record in Explore Bristol Research

PDF-document

Mechatronic Suspension Design for Vehicle Dynamic Performance Enhancement

H. Yuan [1], **Y. Li** [1], **J.Z. Jiang** [1], **P.H. Mellor** [2]
[1] University of Bristol, Department of Mechanical Engineering,
Queen's Building, University Walk, Bristol, United Kingdom

[2] University of Bristol, Department of Eelecitrical and Electronic Engineering,
Merchant Ventures Building, Woodland Road, Bristol, United Kingdom
e-mail: **hy13097@bristol.ac.uk, yl14470@bristol.ac.uk, z.jiang@bristol.ac.uk, P.H.Mellor@bristol.ac.uk**

Abstract
This paper investigates the performance advantages of an mechatronic suspension strut for a road vehicle. Mechatronic struts have attracted growing research interest since the interior electrical circuit has the potential to realise the high-order impedances with sensible size and weight to achieve desirable performance. In addition, to deal with different driving conditions (speed and road roughness, for example) it is much more straightforward to adjust electrical element values in real-time compared with changing pure mechanical elements. To obtain the optimal mechatronic suspension design, a methodology is proposed by considering all possible design parameters and constraints such as nominal voltage and current for the motor maximum force acting on the ball-screw mechanism, and size and weight of the electrical elements. Based on a qualitative analysis of a proposed mechatronic strut, it is concluded that in order to achieve improved performance, the ball-screw needs to have small rotational inertia and large bearable force, and the motor should have small inertia, internal resistance, internal inductance and large nominal current and voltage. This qualitative analysis provides brief guideline for ball-screw and motor selection. Case studies are carried out with a quarter car model using two electrical candidate layouts. They show the potential performance advantages of the mechatronic strut using a motor with sufficiently large nominal current.

1 Introduction

Mechatronic suspension struts attract wide attentions with great potential in realising complex networks and performance enhancement. Different realisations of mechatronic strut have been studied recently. In Sijing's paper [1], two different types of Energy Harvesting Shock Absorbers (EHSAs), one with mechanical motion rectifier (MMR) and one without it, have been compared on different vehicles. It has been shown that MMR-EHSAs provide better rider performances and road handling simultaneously over the traditional shock absorber when installed on light-damped, heavy-duty vehicles. The EHSAs translate the up-and-down suspension vibration into a bidirectional rotation of the generator using a rack-pinion mechanism. A ball-screw mechanism can also be applied to translate linear motion to rotational motion in mechatronic struts, which is presented in [2]. Furthermore, a prototype of an electro-hydraulic semi-active damper was designed and manufactured, and a series of experimental tests were conducted to demonstrate its effectiveness to generate the damping characteristic for enhanced performance in Yuxin's paper [3]. Apart from rotary motors, linear motor is also employed in the mechatronic strut. For example, in Songye's paper [4], a novel application of electromagnetic damper using a linear motor is studied on structural vibration control, and it presents a theoretical and experimental study of linear electromagnetic dampers connected with four representative circuits. A good match between the modelling and testing results clearly demonstrates that the described model can predict the performance of the linear electromagnetic damper very well.

In mechatronic struts, rotary motors are commonly used with a mechanism to translate linear motion to translational such as ball-screw and rack-and-pinion. Rotary motors and these mechanisms bring inertia effects to the strut, which is considered and can be realised as an inerter in a mechanical network. Since the inerter [5] was proposed to substitute the mass element in the mechanical-electrical analogy, the abundant electrical theorems can be directly applied to the analysis and synthesis of mechanical networks which can be used in designing mechanical systems to achieve enhanced performance. The more high-order passive impedance, the further enhanced system performance is obtained [6]. In this analogy, the physical characteristics of inerters, dampers and springs correspond to the electrical characteristics of capacitors, resistors and inductors, respectively. The mechatronic strut, combined of mechanical and electrical networks, can be translated to a equivalent mechanical network using this analogy. The synthesis of a high-order pure mechanical system is difficult due to the limitation on the size and weight of the system. Therefore, in [2], a high-order passive impedance can be easily realised by a basic mechanical network with a high-order electrical network, where a prototype of the mechatronic strut was proposed and applied to vehicle suspension systems. Although considerable research effects have been made, some challenges still exist which hinder the large scale application of mechatronic vibration suppression devices. Firstly, a systematic optimum design approach has not been established to identify the optimum designs for both the mechanical and electrical parts, in terms of the topology and element values. Secondly, realistic considerations, such as weight, size and robustness of the whole system, have not been fully explored.

In this paper, a design methodology for mechatronic struts is presented. Based on qualitative analysis, some guidelines for ball-screw and motor selection are drawn. Case studies have shown that the mechatronic strut has a potential to achieve enhanced performance for road vehicles. This paper is arranged as follows: Section 2 introduces the principles of the mechatronic strut and represents its corresponding mechanical network and admittance function. In Section 3, the design methodology of suspension systems is presented. Furthermore, the qualitative analysis of the mechatronic strut is carried out. Section 4 presents the quarter-car model and the case studies of the mechatronic strut for different motors and suspension networks. In Section 5, some conclusions are drawn.

2 The mechatronic strut

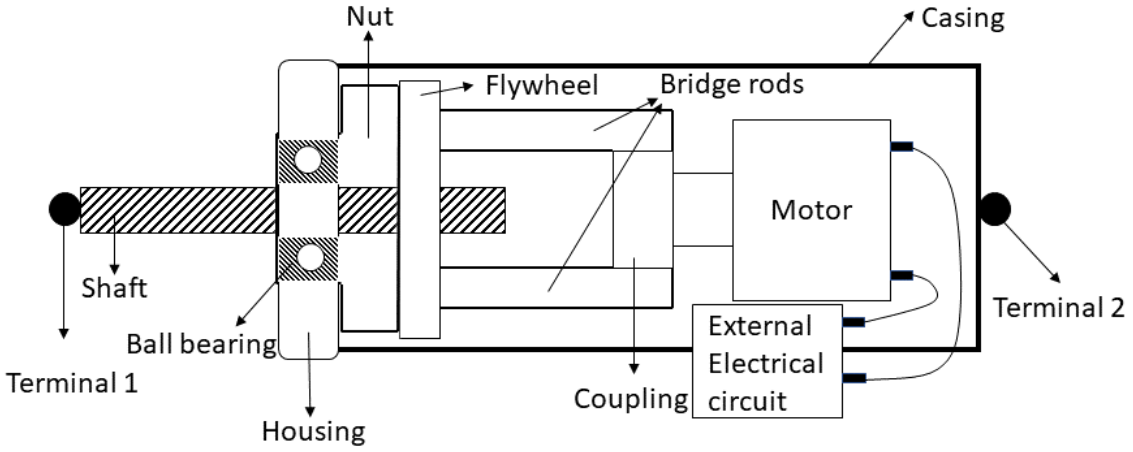

Figure 1: The schematic diagram of the mechatronic strut system

A schematic diagram of the mechatronic strut is shown in Figure 1. The proposed mechatronic strut consists of a ball-screw mechanism, a permanent magnetic electrical motor (PMEM) and an external electrical circuit. The relative linear motion between the two terminals of the strut results in the rotational motion of

the ball-screw mechanism, which in turn drives the motor to generate an inductive voltage. To provide desirable performance, a suitable external electrical circuit is connected to the motor to generate corresponding torque in the rotor. The torque acts back to the ball-screw mechanism, and hence change the force-velocity behaviour across terminals 1 and 2. Furthermore, the external electrical circuit is connected to the PMEM terminals.

The working principle and electrical model of a PMEM is introduced, and then the principle of a ball-screw mechanism is presented. In Section 2.3, the admittance and equivalent mechanical network of the mechatronic strut is introduced.

2.1 The permanent magnet electric motor

In a PMEM, the armature can be modelled as a resistor R_m and inductor L_m in series in electrical circuits. R_m is the coil resistance of the armature and the inductance L_m for the armature is produced once the armature rotates. Figure 2 presents the schematic electrical circuit diagram of a PMEM with an external electrical circuit connected.

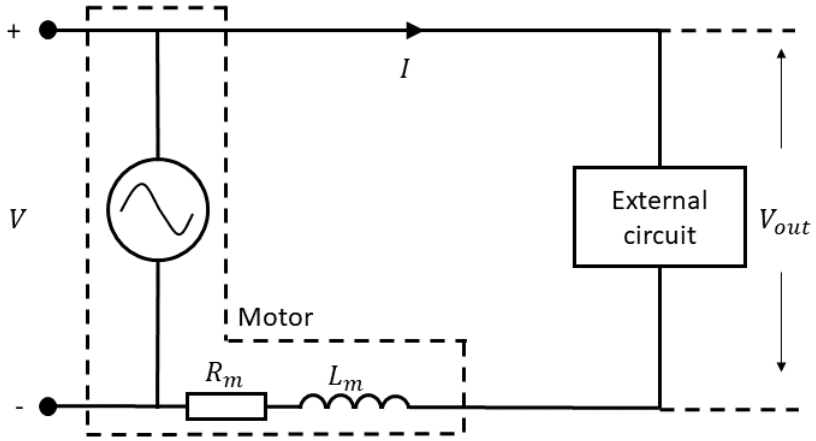

Figure 2: The schematic electrical circuit diagram for a PMEM model connected with an external electrical circuit.

The inductive voltage V and inductive torque T_m are generated by the motor simultaneously while the armature rotates. If the armature rotates with an angular velocity ω, the inductive voltage V can be represented as:

$$V = k_e \cdot \omega, \tag{1}$$

where k_e is the voltage constant (Vs/rad). The armature current I can then be calculated from the inductive voltage V and electrical admittance $Y_e(s)$, with the latter determined by the external electrical circuit and armature model. The expressions of I in the Laplace domain and $Y_e(s)$ are given as follows:

$$\widetilde{I} = Y_e(s) \cdot \widetilde{V}, \tag{2}$$

$$Y_e(s) = \frac{\widetilde{I}}{\widetilde{V}} = \frac{1}{R_m + s \cdot L_m + Z_{ex}(s)}, \tag{3}$$

where $Z_{ex}(s)$ is the external circuit impedance. Then the inductive torque T_m is calculated by the following equation:

$$T_m = k_t \cdot I, \tag{4}$$

where k_t is the motor torque constant with unit $\mathrm{N} \cdot \mathrm{m/A}$. The inductive voltage constant k_e and inductive torque constant k_t are identical and are determined by the magnetic flux, the number of the armature coils and poles of a PMEM. Therefore, the dynamics of the motor in rotational direction can be represented as:

$$T_E = J_m \frac{d\omega}{dt} + T_m + B_m \omega, \tag{5}$$

where T_E is the total torque generated by the motor and J_m the moment of inertia for the rotor. B_m is the damping coefficient of the motor strut.

2.2 Ball-screw mechanism

A ball-screw mechanism is used to convert linear motions into rotational motions to drive the motor. The relation between the force F_M on the ball-screw and the torque T_M is shown as follows:

$$F_M = (\frac{2\pi}{P}) T_M, \tag{6}$$

where P is the pitch of a ball-screw mechanism. The relation between the angular velocity ω on the ball-screw and the linear velocity v is presented as follows:

$$\omega = (\frac{2\pi}{P}) v, \tag{7}$$

If the ball-screw mechanism is ideal, for example, by ignoring friction and backlash, the torque T_M can be expressed as follows:

$$T_M = J_T(\frac{d\omega}{dt}), \tag{8}$$

where J_T is the total moment of inertia of the nut and the flywheel in a ball-screw mechanism, which can produce an inertance effect for the strut. Substituting Equations 7 and 8 into 6, the force F_M is given as:

$$F_M = (\frac{2\pi}{P})^2 J_T(\frac{dv}{dt}) = b \cdot a, \tag{9}$$

where $b = (\frac{2\pi}{P})^2 J_T$ is the ball-screw inertance and a the relative acceleration across its two terminals. The total ball-screw mechanism inertance b can be easily adjusted by tuning the flywheel.

2.3 Mechanical admittance of the mechatronic strut

To determine the admittance and equivalent mechanical network of the mechatronic strut, the dynamics of the motor in rotational direction is transferred to translational direction. As the torque T_E is acting through the ball-screw mechanism to the system, the dynamics of the motor in translation direction can be written by substituting Equation 7 and $F = \frac{2\pi}{P} T$ into Equation 5 and simplified as follows:

$$F_E = \frac{2\pi}{P} T_E = b_e \cdot a + F_m + (\frac{2\pi}{P})^2 B_m v, \tag{10}$$

where F_E is the force produced by the motor, the inertance, b_e, generated by the rotor equals $(\frac{2\pi}{P})^2 J_m$, and the inductive force, F_m, equals $\frac{2\pi}{P} T_m$. The total force F generated by the mechatronic strut is the sum of mechanical force F_M and electrical force F_E as given by:

$$F = F_M + F_E. \tag{11}$$

Substituting Equations 9 and 10 into 11, the dynamics equation of the mechatronic strut can be rewritten as follows:

$$F = (b_e + b) \cdot \frac{dv}{dt} + F_e + (\frac{2\pi}{P})^2 \cdot B_m \cdot v \tag{12}$$

Substituting Equation 1 - 4 and 6 - 7 into Equation 12 to obtain the admittance Y_{ms} of the mechatronic strut:

$$Y_{ms} = \frac{F(s)}{v(s)} = (b_e + b)s + (\frac{2\pi}{P})^2 B_m + \frac{(\frac{2\pi}{P})^2 k_e k_t}{R_m + s \cdot L_m + Z_{ex}(s)} \tag{13}$$

For simplification, the following parameters are defined:

$$\begin{cases} c_e = (\frac{2\pi}{P})^2 B_m \\ G_m = (\frac{2\pi}{P})^2 k_t k_e \end{cases}$$

Therefore, Equation 13 can be rewritten as follows:

$$Y_{ms} = (b_e + b)s + c_e + \frac{G_m}{R_m + sL_m + Z_{ex}(s)}. \tag{14}$$

From the admittance Y_{ms}, the mechatronic strut can be divided into two parts: the first part $(b_e + b)s + c_e$ is considered as the mechanical inerter and damper of the motor structure, and $G_m/(R_m + sL_m + Z_{ex}(s))$ is regarded as the admittance of an external electrical circuit and motor. Using the analogy of mechanical and electrical systems, the equivalent mechanical network of the strut is presented in Figure 3, where k_m, c_m and G_m/Z_{ex} represent the corresponding internal inductor, internal resistor and external circuit, respectively. The corresponding relationships between electrical and mechanical elements are presented as follows:

$$\begin{cases} k_m = \frac{G_m}{L_m} \\ c_m = \frac{G_m}{R_m} \end{cases}$$

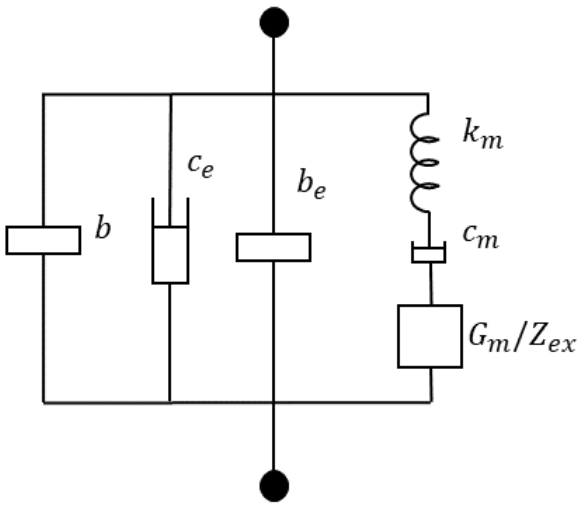

Figure 3: Simplified equivalent network for the mechatronic strut

3 Suspension design

3.1 Optimisation methodology

In the optimisation methodology, design parameters and physical constraints for the ball-screw mechanism, electrical motor and electrical elements are considered. These design parameters and constraints for the strut are listed in Table 1.

	Ball-screw	Motor	Electrical elements
Design parameters	P, J_M	$k_e, k_t, J_m, B_m, R_m, L_m$	R, L, C
Constraints	$\delta x_{max}, F_{max}, b$	$V_{peak}, I_{rms}, \omega$	physical range of c, k, b

Table 1: Selected parameters and constraints considered for the optimisation process.

For a ball-screw mechanism, pitch P is one of the most important design parameters as analysed in Section 2.2 and 2.3. Furthermore, the nut inertia, J_M is another design parameter to represent the minimum inertia of a ball-screw mechanism. As the values of P and J_M is interact, the corresponding J_M for each value of P is different. For a motor, parameters $k_e, k_t, J_m, B_m, R_m, L_m$ are constant properties, but values of them may vary for different motors and can be found from its specification. Based on these parameters and pitch, the value of mechanical elements b_e, k_m and c_m are determined for the mechanical network. In the external circuit, three basic electrical elements may be used which are resistors R, inductors L and capacitors C. The values of their corresponding mechanical elements can be determined from the relations shown as follows:

$$\begin{cases} k = \frac{G_m}{L} \\ c = \frac{G_m}{R} \\ b = G_m \cdot C. \end{cases}$$

Physical constraints for the mechatronic strut have to be determined and implemented into the optimisation process to check if the optimal values of these elements are feasible in physical realisation. For a ball-screw mechanism, δx_{max} and F_{max} are the maximum relative displacement between two terminals and maximum force applied to the ball-screw mechanism, respectively. In the specification, the maximum force F_{max} of a ball-screw mechanism is listed for each set value of P. The minimum inertia of a ball-screw mechanism J_M produces a minimum inertance for the system, which is used as the lower boundary of b for the ball-screw mechanism. If the optimal value of b is bigger than the lower boundary, the rest inertance can be easily adjusted by tuning the attached flywheel. For a motor, to make sure the mechatronic strut system working normally in a long time, the value of V, I and ω calculated in the optimisation process for the motor have to be smaller than its nominal voltage V_{nom}, current I_{nom} and velocity ω_{nom}, respectively. For physical realisation, each electrical element should be considered within its achievable physical range. From these ranges, the constraints for their corresponding mechanical elements can be calculated. Therefore, these constraints are used in the optimisation to obtain the optimum values for these corresponding mechanical elements and meet the physical realisation requirements of electrical elements.

The optimisation methodology can be simplified as some design parameters and constraints may not able to be determined from their specifications. The simplified optimisation methodology is used to for the case studies later on. For motors used in case studies, the damping coefficient B_m is not able in their specifications. Therefore, the value of c_e can not be calculated for the suspension network, and then the element c_e is neglected for the optimisation process. However, the value of B_m can be identified through experiment and implemented into the system. Moreover, it is assumed that all values of electrical elements can be physically realised in the optimisation so the constraints of electrical elements can be neglected in optimisation. Therefore, the general network can be simplified as in Figure 3 without c_e.

3.2 Qualitative analysis

In this section, it provides an analysis to qualitatively discuss what the preferred properties required of the ball-screw mechanism and motor for the mechatronic strut.

3.2.1 Ball-screw mechanism

The total ball-screw inertance $b = b_M + b_{flywheel}$ can be adjusted by adding or removing the flywheel, but there is a lower boundary, which is the inertance b_M dominated by the nut with inertia J_M and pitch P for a ball-screw mechanism and the relation between them is given as follows:

$$b_M = (\frac{2\pi}{P})^2 \cdot J_M \tag{15}$$

Therefore, the total equivalent inertance b_{total} of the mechatronic strut should be larger than b_M and the relation is presented as follows:

$$b_{total} \geq b_M \tag{16}$$

To increase the possibility of achieving more admittance functions for the strut, the value of b_M should be as small as possible only considering the ball-screw mechanism. To have small b_M, the ball-screw mechanism requires large P and small J_M. However, there is a trade-off between pitch P and lower boundary inertia J_M. Sometimes, there is no detailed information available on the trade-off, a specific ball-screw for case studies in Section 4 is picked. Furthermore, the constraint of F_{max} should be as large as possible to enhance the capability of force acting through the ball-screw shaft.

3.2.2 Electrical motor

Inertance b_e in Figure 3, which is fixed once the motor is selected, is dominated by the motor inertia J_m and pitch P and its relation is given as follows:

$$b_e = (\frac{2\pi}{P})^2 \cdot J_m \tag{17}$$

Therefore, combining Equations 15 and 17, b_{total} should be larger than the sum of b_M and b_e and its relation is shown as follows:

$$b_{total} \geq b_M + b_e \tag{18}$$

To increase the possibility of achieving more admittance functions for the strut, the value of b_e should be as small as possible. As b_e is determined by Equation 17, it shows that the large pitch it has with small inetias J_m, the small b_e it will have. Conclusively, the selected motor should have a small inertia to achieve small inertance b_e for a mechatronic strut.

The internal resistance R_m and internal inductance L_m of the selected motor is modelled as a spring k_m and damper c_m in mechanical network which are in series with an external circuit shown in Figure 3. From Equation 3, to increase possibility of obtaining optimum transfer function for a system, the value of R_m and L_m should be as small as possible. For that reason, the values of c_m and k_m should be as large as possible to demonstrate this by applying translation relationships between mechanical and electrical elements. Conclusively, small values of R_m and L_m of a motor is more suitable for the proposed mechatronic strut.

In Section 2.3, the inductive force F_m equals $\frac{2\pi}{P}T_m$. By substituting it into Equation 4, the relation of F_m and I is given as follow:

$$I_{nom} \geq I = \frac{F_m \cdot P}{2\pi \cdot k_t}. \tag{19}$$

From Equation 1 and 7, the relation of V and v is given:

$$V_{nom} \geq V = 2\pi \frac{k_e}{P} v. \tag{20}$$

For each motor, there is a set of corresponding nominal voltage V_{nom} and current I_{nom}. To make sure the optimisation results are feasible, the optimised voltage and current in the electrical circuit must meet these constraints of nominal voltage and current. Furthermore, it is assumed that all optimised electrical elements' values can be realised. Then Equations 19 and 20 can be combined and rearranged as follows:

$$\frac{F_m}{2\pi \cdot I_{nom}} \leq \frac{k_e}{P} \leq \frac{V_{nom}}{2\pi \cdot v} \tag{21}$$

To expand the possible solutions of $\frac{k_e}{P}$, the nominal voltage and current of a motor have to be as large as possible. In conclusion, a optimum motor for the proposed mechatronic strut should have small inertia J_m, internal resistance R_m, internal inductance L_m and large nominal voltage V_{nom} and current I_{nom}.

4 Case studies

The potential performance in ride comfort J_1 of the mechatronic strut is presented in a quarter-car model. A commonly used ball-screw mechanism is selected for the mechatronic strut. Using simplified optimisation procedure, case studies are carried out with specific motors and candidate external electrical circuits.

4.1 Quarter-car model and Performance index

A quarter-car model in Figure 4 (a) is applied to illustrate the performance benefits of the proposed mechatronic strut for vehicle dynamics, where m_s and m_u are the sprung and unsprung masses, x_r the displacement of road excitation, x_s and x_u the corresponding displacement of the sprung and unsprung masses, k_t the tyre stiffness. Figure 4 (b) presents the conventional suspension system for the quarter-car model. In this paper, the parameters of the quarter-car model are fixed as follows: $m_s = 250$kg, $m_u = 35$kg, $k_t = 150$kN/m [7]. Furthermore, $k_s = 30000\mathrm{N/m}$ is set to represent a normal passenger vehicle.

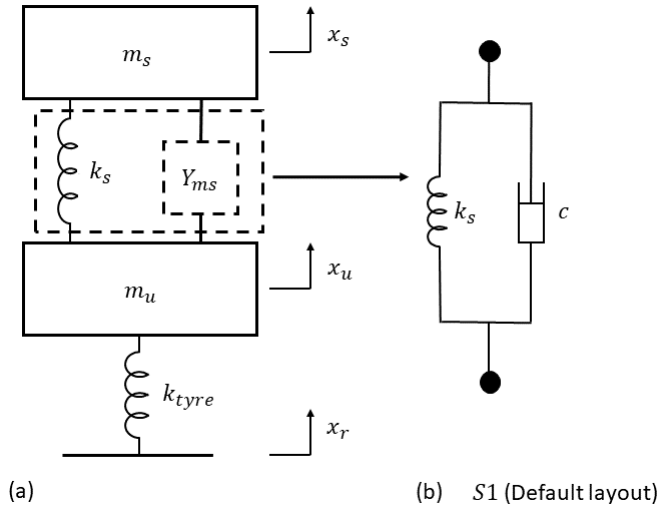

Figure 4: The schematic diagram of the quarter-car model.

To design a suspension system, there are a number of practical design requirements to meet such as passenger comfort, handling, tyre normal loads, limits on suspension travel etc. Although suspension design usually involve a trade-off between various performance requirements, it is useful to consider first how much improvement can be obtained in individual performance measures for various configurations. To compare the performance benefits, ride comfort J_1 index is selected as follows [7]:

$$J_1 = 2\pi\sqrt{V\kappa}||sT_{\widetilde{x}_r \to \widetilde{x}_s}||_2 \tag{22}$$

where $||sT_{\widetilde{x}_r \to \widetilde{x}_s}||_2$ is the H_2 - norm of $sT_{\widetilde{x}_r \to \widetilde{x}_s}$, V the driving velocity of the vehicle, while κ is the road roughness parameter. Values of V and κ are referred in [7].

The road input in time domain is also used to determine the system transient response such as V_{peak} and I_{rms}. The procedure to generate the time domain signal is referred in [8].

4.2 Selected ball-screw

Based on qualitative analysis, the ball-screw mechanism should have small inertia and large force constraints. In Yilun's paper [9], a common ball-screw mechanism, which the inertia and pitch are $0.02\mathrm{kgcm}^2$ and $6\mathrm{mm}$, respectively, is was proposed for a novel shock absorber. The value of maximum force constraint was not presented in Yilun's paper so it is taken from common ball-screw mechanism specification where its value is $26.5\mathrm{kN}$ [10].

4.3 Selected motors

The qualitative analysis in Section 3.2 gives a brief guidelines for motor selection. Furthermore, the maximum terminal voltage of motors must be below $48\mathrm{V}$ considering automotive $48\mathrm{V}$ system [11]. As a result, two specific motors are selected with maximum available terminal voltage (48 V) and their parameter values are presented in Table 2. Comparing Motor-1 and Motor-2, Motor-1 has a small inertia J_m while Motor-2 has large nominal I and small R_m and L_m. Two candidate external electrical circuits E_1 and E_2 are proposed, with the corresponding mechanical networks shown in Figure 5. The proposed two electrical circuits are used to replace the G_m/Z_e part in Figure 3.

	$V_{nom}(\mathrm{V})$	$I_{nom}(\mathrm{A})$	$R_m(\Omega)$	$L_m(\mathrm{mH})$	$J_m(\mathrm{gcm}^2)$	$k_t(\mathrm{Nm/A})$	$k_e(\mathrm{Vs/rad})$
Motor-1	48	1.41	2.95	0.514	21.2	0.0429	0.0428
Motor-2	48	2.17	1.40	0.473	75.9	0.0585	0.0586

Table 2: Parameters values for different motors.

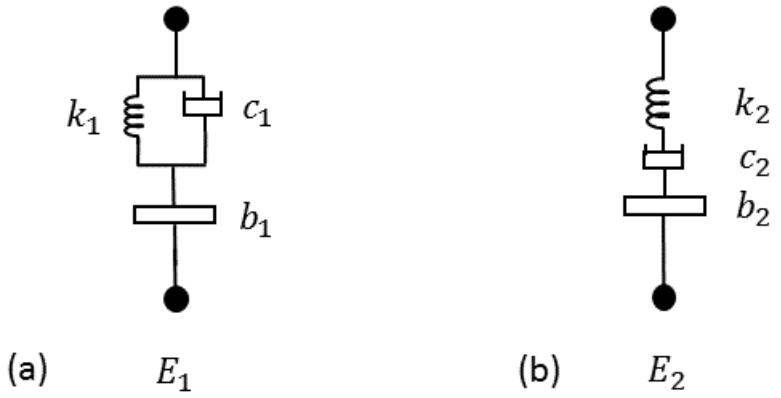

Figure 5: The corresponding mechanical networks of two external electrical circuits E_1 and E_2.

Table 3 shows the optimisation results of four cases for two different motors in two different suspension networks using E_1 and E_2. In comparison with the optimal J_1 obtained by the conventional suspension

network S_1 shown in Figure 4 (b), the dynamic performance J_1 of four cases are much worse. It also can be seen from Table 3 that current in motors reaches the upper boundary of constraints I_{nom} for all cases. To explore the impacts of the constraints on the cost function, a further investigation of J_1 to the change of constraint values is necessary. As the terminal voltage of motors has not reached the safe level, here only the constraint I_{nom} is considered.

	J_1			V_{peak}(V)		I_{rms}(A)	
	Optimal, S_1	E_1	E_2	E_1	E_2	E_1	E_2
Motor-1	1.24	41.4	41.4	10.6	10.8	1.41	1.41
Motor-2	1.24	27.2	12.6	13.2	41.2	2.17	2.17

Table 3: Results of two different motors.

If the constraint I_{nom} is released for both specific motors, the optimal J_1 can be further improved. Table 4 presents the optimal results of J_1 and their corresponding required current I_{rms} and voltage V_{peak} in the electrical circuit for all cases. In comparison with the optimal J_1 obtained by the conventional suspension system S_1, a maximum 14.5 % enhanced performance in ride comfort can be achieved if I_{nom} of Motor-2 using network E_1 is large enough. Furthermore, a 13.7% improvement of J_1 is obtained with Motor-2 using network E_2. Comparing these two cases, Motor-2 using E_1 is better for the system as it has smaller required current and larger improvement. As improvements for Motor-1 using both networks are poor, Motor-2 with large I_{nom} and small R_m and L_m is more suitable the system.

Figure 6 presents the vertical acceleration of m_s in frequency domain for all cases. Furthermore, the vertical acceleration of m_s in time domain for the optimal case is shown in Figure 7 where only 25s response signal is shown. To clearly see improvements in time and frequency domain, the response of vertical acceleration of m_s is presented in both domains.

In conclusion, for these two specific motors, none of them can provide a better dynamic performance J_1 than the optimised conventional system. However, the investigation of constraint I_{nom} shows that both motors with large I_{nom} can obtain better dynamic performance J_1. Furthermore, Motor-2 with smaller internal resistance and inductance and large nominal current can have better performance.

	Optimal, S_1	Motor-1, E_1	Motor-1, E_2	Motor-2, E_1	Motor-2, E_2
J_1	1.24	1.23	1.23	1.06	1.07
I_{rms}(A)	-	3.3	3.4	3.4	4.1
V_{peak}(V)	-	48	48	48	48
Improvement (%)	-	0.8	0.8	14.5	13.7

Table 4: Optimal results of J_1 for four cases and their corresponding required current, voltage and improvement.

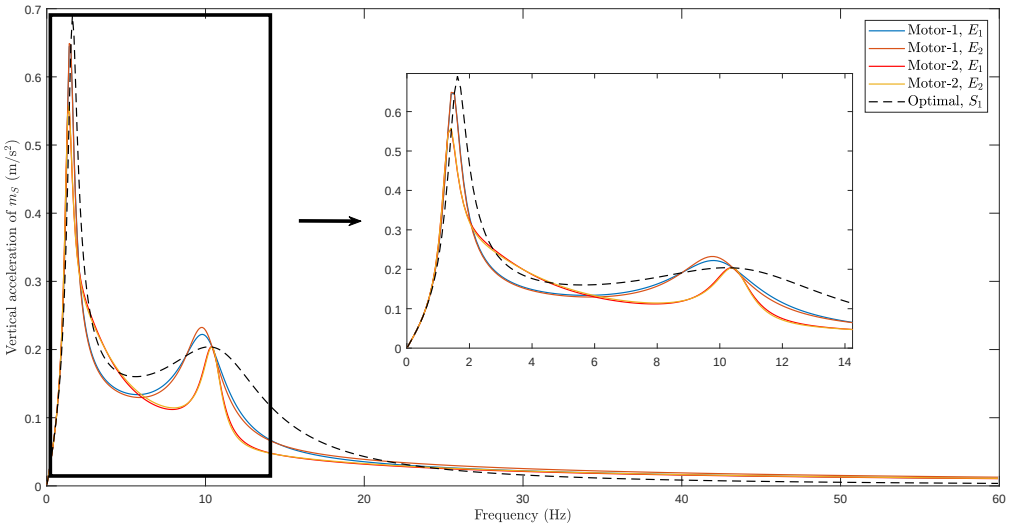

Figure 6: The vertical acceleration of m_s in frequency domain.

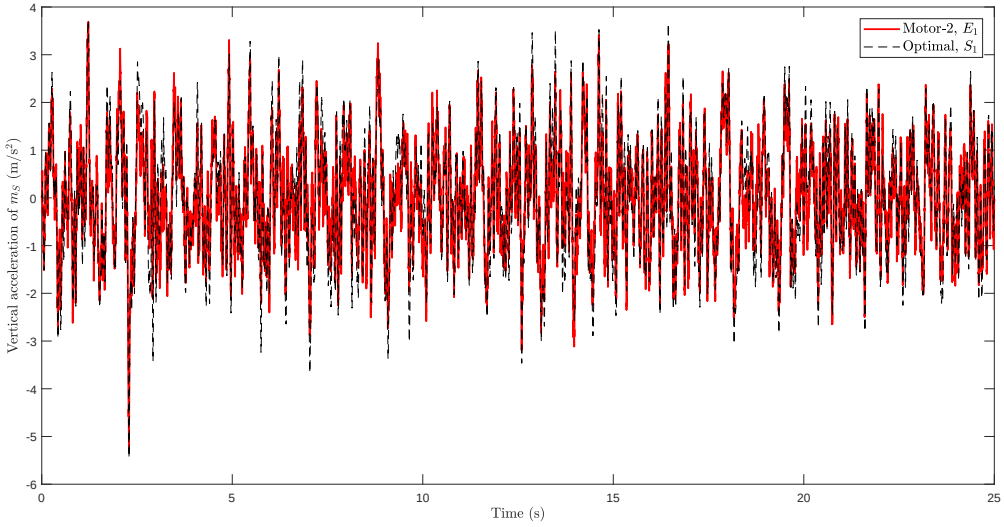

Figure 7: The vertical acceleration of m_s in time domain.

5 Conclusion

This paper investigated the potential of mechatronic strut for road vehicles and proposed a design methodology and qualitative analysis. Cases studies of the mechatronic vehicle suspension strut were carried out and it shows that the strut can provide improvements of ride comfort for a quarter-car model. To obtain the optimal mechatronic suspension design, an optimisation methodology is proposed by considering all possible design parameters and constraints such as nominal voltage and current for the motor, maximum force acting on the ball-screw mechanism and size and weight of the electrical elements. In the qualitative analysis of the mechantronic strut, an motor for the strut should have small inertia J_m, internal resistance R_m, internal inductance L_m and large nominal current I_{nom} and voltage V_{nom}. A ball-screw mechanism should have small initial inertance b_M and large bearable force F_{max}. Furthermore, to obtain the optimal J_1 for the system, the

corresponding suitable ratio of $\frac{k_e}{P}$ can be only a value or within a range. Therefore, there may be multiple solutions of $\frac{k_e}{P}$ for the system. Simultaneously, there are multiple available choices for motor and ball-screw mechanism selections for each value of $\frac{k_e}{P}$. In case studies, the dynamic performance of suspensions using two specific motors are determined with two candidates external electrical circuits by using a simplified optimisation procedure. It shows obtained J_1 for all these motors are worse than J_1 obtained by conventional suspension system. This is because that J_1 becomes poor to meet those constraints in optimisation such as I_{nom} and V_{nom}. Then the impact of I_{nom} to J_1 was carried out as V_{nom} has not reached the safe level shown in Table 4. From the analysis for both motors, dynamic performance J_1 can be improved significantly if the constraint of I_{nom} is released. As Motor-2 has small internal resistance and inductance, optimal J_1 obtained using Motor-2 is better than that obtained with Motor-1 with up to 14.5% improvement.

Acknowledgements

The authors would like to acknowledge the support of the Royal Society, EPSRC and the China Scholarship Council: Jason Zheng Jiang is supported by an Royal Society (Reference: IE151194) and EPSRC grants (Reference: EP/P013456/1), Hui Yuan is supported by an EPSRC scholarship (Reference: EP/N509619/1) and Yuan Li is supported by a China Scholarship Council studentship.

References

[1] S. Guo, Y. Liu, L. Xu, X. Guo, and L. Zuo, *Performance evaluation and parameter sensitivity of energy-harvesting shock absorbers on different vehicles*, Vehicle System Dynamics, Vol. 54, No. 7, (2016), pp.918-942.

[2] F. C. Wang, H. Chan, *Vehicle suspensions with a mechatronic network strut*, Vehicle System Dynamics, Vol. 49, No. 5, (2011), pp. 811-830.

[3] Y. Zhang, H. Chen, K. Gao, X. Zhang, and S. E. Li, *Electro-hydraulic damper for energy harvesting suspension: Modeling, prototyping and experimental validation*, Applied energy, Vol. 199, (2017), pp. 1-12.

[4] S. Zhu, W. A. Shen, and Y. L. Xu, *Linear electromagnetic devices for vibration damping and energy harvesting: Modeling and testing*, Engineering Structures, Vol. 34, (2012), pp. 198-212.

[5] M. C. Smith, *Synthesis of mechanical networks: The inerter*, IEEE Transactions on automatic control, Vol. 47, No. 10, (2002), pp. 1648-1662.

[6] C. Papageorgiou, M. C. Smith, *Positive real synthesis using matrix inequalities for mechanical networks: application to vehicle suspension*, IEEE Transactions on Control Systems Technology, Vol. 14, No.3, (2006), pp. 423-425.

[7] M. C. Smith, and F. C. Wang, *Performance benefits in passive vehicle suspensions employing inerters*, Vehicle System Dynamics, Vol. 42, No. 4, (2004), pp. 235-257.

[8] J. Z. Jiang, A. Z. Matamoros-Sanchez, A. Zolotas, R. M. Goodall, and M. C. Smith, *Passive suspensions for ride quality improvement of two-axle railway vehicles*, Proceedings of the Institution of Mechanical Engineers, Part F: Journal of Rail and Rapid Transit, Vol. 229, No. 3, (2015), pp.315-329.

[9] Y. Liu, L. Xu, and L. Zuo, *Design, Modeling, Lab, and Field Tests of a Mechanical-Motion-Rectifier-Based Energy Harvester Using a Ball-Screw Mechanism*, IEEE/ASME Transactions on Mechatronics, Vol. 22, (2017), pp. 1933-1943.

[10] THK CO., LTD, *Precision Ball Screws DIN Standard Compliant Ball Screw*, https://tech.thk.com/upload/catalog_claim/pdf/335-2E.pdf, Access on 5th May 2018.

[11] M. Bikson, *A review of hazards associated with exposure to low voltages* New York: University of New York, (2004).